Radiation Torque and Force on Optically Trapped Linear Nanostructures

F. Borghese,* P. Denti, and R. Saija
Dipartimento di Fisica della Materia e Tecnologie Fisiche Avanzate, Università di Messina, Salita Sperone 31, 98166 Messina, Italy

M. A. Iatì and O. M. Maragò†
Istituto per i Processi Chimico-Fisici (Messina), Consiglio Nazionale delle Ricerche, Salita Sperone, 98158 Faro Superiore, Messina, Italy

(Received 7 January 2008; published 22 April 2008)

We study the optical trapping of highly elongated linear nanostructures in the focal region of a high-numerical aperture lens (optical tweezers). The radiation torque and trapping force on these nanostructures that are modeled as chains of identical spherical scatterers are calculated by means of multipole field expansions in the framework of the transition matrix approach. We investigate both orientational and trapping stability and calculate force constants and trap parameters in order to clarify the role of the linear geometry in the optical trapping mechanism. Furthermore, we calculate optical trapping of nanowires of different materials and compare our theoretical findings with available experimental results.

DOI: 10.1103/PhysRevLett.100.163903 PACS numbers: 42.50.Wk, 42.25.Fx, 62.23.Hj

Optical tweezers [1] are commonly used tools in both physical [2] and life sciences [3] for manipulating matter from the micron to the atomic scale and as force transducers in the picoNewton range [4,5]. Very recently, optical trapping, manipulation, and assembling of quasi-1D nanostructures, such as semiconductor nanowires [6–8] and carbon nanotubes [9–12], were achieved in aqueous environments. The almost linear geometry of nanowires with a subwavelength cross section and very high aspect ratio is of fundamental importance for bridging the gap between the microworld and the nanoworld [13,14]. Furthermore, their potential use for a new kind of scanning probe microscopy and spectroscopy has also been demonstrated [8]. However, for these applications to take hold it is of fundamental importance to understand the optical trapping properties of quasi-1D nanostructures, to evaluate quantitatively radiation force and torque acting on them, and eventually to shed light on their dynamics in the optical trap. Only recently theoretical calculations on optically trapped latex spheres have shown a quantitative agreement with experiments even when the particle size is close to the radiation wavelength [15,16]. Here, we use our recent reformulation of the optical trapping [16] and of the radiation torque [17] to investigate the behavior of trapped linear nanostructures, to discuss their orientational and trapping stability, and to calculate the force constants for a number of materials of practical interest.

Theory.—The formalism that we devised to describe the radiation force and torque on nonspherical particles [16,17] makes full use of the Maxwell stress tensor [18] in which the fields are the superposition of the field incident on the particles and of the field scattered by the particles themselves. Both these fields are expanded in a series of vector spherical multipole fields [19], in terms of whose amplitudes all the quantities of interest are given. The multipole amplitudes of the scattered field are calculated from those of the incident field through the transition matrix approach [20] that applies to particles of any shape, even of high aspect ratio, and resorts to the only approximation of truncating the series after a number of terms sufficient to ensure fair convergence of all the quantities of interest. A comprehensive description of this technique applied to particles modeled as aggregates of spheres can be found in [21–23].

Geometry.—In our study we consider an optical system typical of optical tweezers experiments (see Fig. 1). We assume an aplanatic system whose optical axis coincides with the z axis of a rectangular coordinate system; the nominal focus F of the lens is located at the origin O. The back focal plane is illuminated by a TEM_{00} Gaussian beam, linearly polarized along the x axis and propagating in the positive direction of the z axis, with filling factor $f_0 = 2$ [24] and wavelength $\lambda_0 = 1064$ nm *in vacuo*, i.e., $\lambda = 800$ nm in water. The numerical aperture of the lens is N.A. $= 1.2$, and the exit pupil is immersed in oil with refractive index $n = 1.52$ whereas the trapped particles are immersed in water ($n = 1.33$). Oil and water are sepa-

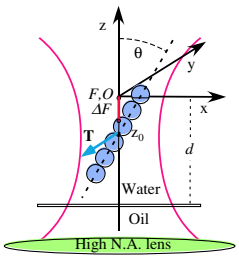

FIG. 1 (color online). Sketch of the geometry of the optical trap for a x-polarized TEM_{00} laser beam propagating in the positive direction of the z axis. The vector **T** represents the radiation torque exerted on the chain trapped at z_0 with its axis in the xz plane.

rated by a cover slip, orthogonal to the optical axis, located at $d = -20$ μm with respect to the origin. Because of the spherical aberration caused by the presence of two media of different refractive index, the maximum field intensity, yet on the optical axis [24], is shifted from F by $\Delta F = -4.0$ μm [25].

Modeling linear nanostructures.—The particles we deal with are modeled as linear chains of length L composed of identical spheres of diameter D. The L and D values we choose prove convenient in highlighting the orientational behavior of the chains, as we will show below. Moreover, we investigate long chains (up to 20 spheres) with $D = 50$ nm in order to compare our calculated results with some experimental data available for semiconductor nanowires [7,8]. In fact, the $D = 50$ nm spheres are much smaller than the wavelength, so that these chains are a good model for quasi-1D nanostructures [23,26]. At first we consider linear chains composed of latex spheres (refractive index $n_p = 1.57$), with diameter 220, 100, and 50 nm. Then, we consider linear chains of 20 identical spheres with diameter 50 nm composed of various semiconducting materials. We calculate for each chain the radiation force $\mathbf{F}_{\text{rad}}(\mathbf{r})$, the argument $\mathbf{r}$ denoting the position of the center of mass of the chain. The trapping occurs on the optical axis [25] where all the components of $\mathbf{F}_{\text{rad}}(\mathbf{r})$ vanish with a negative derivative. In the vicinity of the trapping point $\mathbf{r}_0 \equiv (0, 0, z_0)$ the components of $\mathbf{F}_{\text{rad}}(\mathbf{r})$ can be approximated by

$$F_{\text{rad }x}(x, 0, z_0) = -\kappa_x x, \qquad F_{\text{rad }y}(0, y, z_0) = -\kappa_y y, \qquad F_{\text{rad }z}(0, 0, z) = -\kappa_z (z - z_0), \tag{1}$$

where κ_x, κ_y, and κ_z are the stiffness constants. The orientation of the aggregates is individuated by the polar angles ϑ and φ of the axis of the linear chain. For each orientation we determined first the trapping position of the center of mass of the chain, then calculated the torque $\mathbf{\Gamma}_{\text{rad}}$ at that position. As regards the torque, we actually calculate the adimensional vector

$$\mathbf{T} = \frac{16\pi^2}{n^2 \lambda |E_0|^2 \sigma_{\text{T}}} \mathbf{\Gamma}_{\text{rad}},$$

where E_0 is the amplitude of the incident field, σ_{T} is the extinction cross section of the chain, and $n = 1.33$. The orientational stability occurs when the Cartesian components of $\mathbf{T}$ vanish with a negative derivative with respect to both ϑ and φ. In this respect we notice that in all the cases we dealt with the components T_x and T_z vanish (with negative derivatives) when the chain lies in the xz plane, i.e., when $\varphi = 0$. In other words, the xz plane is a plane of orientational stability with respect to φ, as expected on account of the symmetry of the chains and of the polarization of the incident beam. Accordingly, in all the following figures we assume $\varphi = 0$. On this assumption, when $T_y < 0$ the chains are forced to align to the optical axis, whereas when $T_y > 0$ they tend to align along the polarization axis.

Results for latex chains.—Let us first consider the linear chains composed of 2, 3, and 6 latex spheres of diameter 220 nm. In Fig. 2(a) we report the trapping position as a function of ϑ for all the chains. Even a cursory examination shows that the trapping position is strongly dependent on the tilt angle and that the 6-spheres chains are not trapped for $\vartheta > 70°$. It is tempting to attribute this result to the length of these chains ($L = 1.32$ μm) that exceeds the width of the trapping spot (≈ 800 nm). Nevertheless, we will show below that chains with a length of 1 μm and diameter of 50 nm do trap even when orthogonal to the optical axis ($\vartheta = 90°$). In this respect, we remark that σ_{T}, the extinction cross section of the particles, depends on their orientation and that the dominant term in $F_{\text{rad }z}$, the component of the radiation force along the optical axis, is proportional just to σ_{T} [27]. Now, our calculations show that, at any tilt angle, the extinction cross section of the 220 nm chains is about 1000 times larger than that of the 50 nm chains. Therefore, $F_{\text{rad }z}$ may grow so large as to prevent the trapping of the 220 nm chains for $\vartheta > 70°$. However, the curves in Fig. 2(b) show that $T_y < 0$ so that the torque forces the chains to align their axis to the optical axis, the strongest torque being exerted just on the 6-spheres chains.

The chains of diameter 100 nm include up to 6 spheres and thus their maximum length is 600 nm, whereas those with a diameter of 50 nm include up to 20 spheres with a maximum length of 1 μm. We first state that all the chains of 100 nm spheres undergo trapping, whatever their tilt angle, and that the trapping position is almost independent of ϑ. Moreover, Fig. 3(a), in which we report T_y as a function of ϑ for these chains, shows that for the 2-spheres chains $T_y > 0$, whereas $T_y < 0$ for the 6-spheres chains. Thus, the shorter chains tend to orient along the polariza-

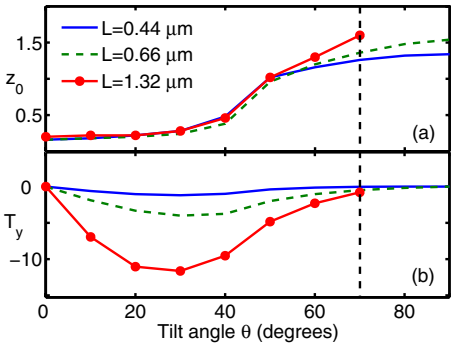

FIG. 2 (color online). Calculated trapping position z_0 (μm) (a) and T_y (b) as a function of the tilt angle ϑ for chains of spheres of latex with diameter $D = 220$ nm and lengths $L = 0.44$ (2 spheres), 0.66 (3 spheres), and 1.32 μm (6 spheres). In (a) the origin of the z axis is shifted by ΔF. The vertical dashed line marks the tilt beyond which the 6-spheres chains do not trap.

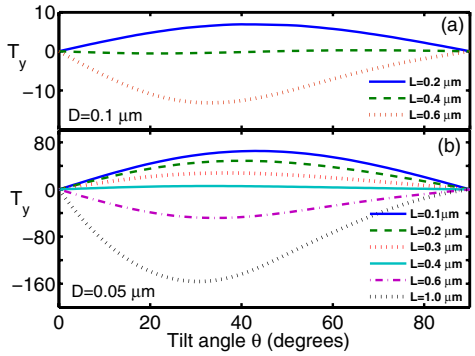

FIG. 3 (color online). Calculated T_y as a function of the tilt angle ϑ for several values of the length L of the chains of latex spheres with diameter $D = 100$ nm in (a) and 50 nm in (b).

tion axis, whereas the longer ones tend to align with the optical axis. The chains with $L = 400$ nm mark a change in the sign of T_y, hence a change in the orientational stability. The behavior of the chains with a diameter of 50 nm is quite analogous; i.e., whatever their length, they undergo trapping. According to Fig. 3(b), in which we report T_y as a function of ϑ, for the shorter chains $T_y > 0$, whereas for the longer ones $T_y < 0$. The point of inversion lies somewhere between the 8- and the 9-spheres chains, i.e., at $L \approx 400$ nm.

The properties of the 50 nm chains have been further investigated by reporting in Fig. 4 the force constants as a function of L [25] for $\vartheta = 90°$ in 4(a) and for $\vartheta = 0°$ in 4(b). In the case of alignment along the optical axis ($\vartheta = 0°$) the force constants scale linearly with L. This dependence is in agreement with the preliminary results of Pauzauskie *et al.* [7] who measured the stiffness κ_z for GaN nanowires of various length.

In Fig. 5 we report the polarization asymmetry $1 - \kappa_x/\kappa_y$ [5(a)] and the geometric asymmetry $(\kappa_x + \kappa_y)/2\kappa_z$ [5(b)] as a function of L. On account of the

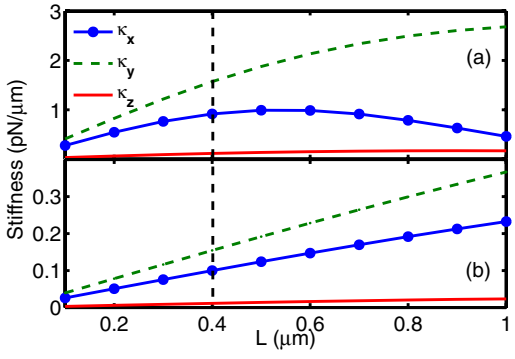

FIG. 4 (color online). Trap stiffnesses as a function of the length L of linear chains of latex spheres of diameter $D = 50$ nm with their axis along the x axis (a) and along the z axis (b). The vertical dashed line marks the value of L where the orientational behavior changes.

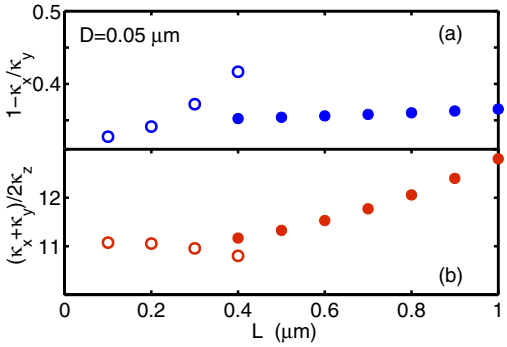

FIG. 5 (color online). Polarization asymmetry (a) and geometrical asymmetry (b) factors calculated in the stable orientation as a function of L for chains of latex spheres with $D = 50$ nm. For $L \leq 0.4$ μm the results are for alignment along the x axis, for $L \geq 0.4$ μm the alignment is along the optical axis.

calculated different behavior of long and short chains, for $L \leq 0.4$ μm we report the results for alignment along the polarization axis, whereas for $L \geq 0.4$ μm the reported results are those for alignment along the optical axis. Both graphs show a sharp discontinuity, also in slope, at $L = 0.4$ μm, i.e., at the length where T_y changes its sign.

Results for chains of other materials.—The calculations on latex chains, especially the longest ones, gave enough information to make us able to understand the behavior of chains of other materials for which experimental data are available. We considered chains of 20 identical spheres with diameter 50 nm composed of ZnO, $KNbO_3$, GaN, and Si, all trapped and oriented along the optical axis, in agreement with our previous findings and with the experimental observations [7,8]. We also found that the stiffness κ_z is a linear function of the laser power, in agreement with the experimental results by Pauzauskie *et al.* [7] for GaN nanowires of various lengths. It is interesting that the trapping parameters that we calculated for all the chains and report in Fig. 6 depend linearly on the refractive index. The parameters for latex chains are also reported for the sake of comparison. Indeed, we attempted to calculate the

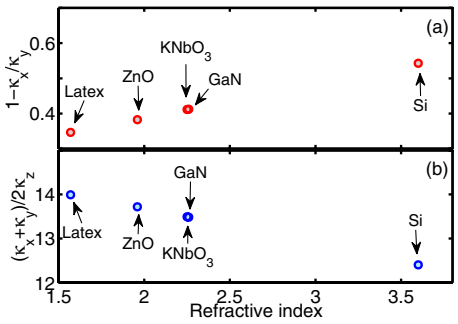

FIG. 6 (color online). Calculated polarization asymmetry factors (a) and geometric asymmetry factors (b) versus the refractive index for chains of 20 spheres with $D = 50$ nm. The orientation of all the chains is along the optical axis.

corresponding quantities for chains of Ag, but no result is reported because, in agreement with the experiment [7], the metallic (complex) index of refraction prevents the trapping.

Conclusions.—The results discussed above show that the trapping of linear chains presents features that are akin to those observed for trapped nanowires. According to our calculations, the trapping position, if any, does not depend only on the aspect ratio, but also on the diameter of the component spheres. Actually, the 6-spheres chains with a diameter of 220 nm do not trap when their tilt angle is too large. Nevertheless, due to the strong radiation torque, they are forced to become parallel to the optical axis and in this configuration they do trap. If this situation were due to the aspect ratio only, a similar behavior should be expected for the 6-spheres chains with a diameter of 100 and 50 nm. On the contrary, these chains do trap for any tilt angle and, in particular, the 50 nm chains do trap even when their aspect ratio is as high as 20:1 (20-spheres chains). We already stressed that the lack of trapping of the 6-spheres, 220 nm chains cannot be due only to the fact that their length exceeds the size of the trapping spot, explaining the reasons for which it is not surprising that the thickest chains do not trap for large values of the tilt angle.

According to our calculations, the trapping position depends on the orientation of the chain, that, in turn, depends on the length. In fact, on account of the radiative torque they undergo, the shortest chains are stably oriented transversely to the optical axis, whereas the longest ones dispose themselves along the optical axis.

We calculated force constants and torque for long chains of several materials finding qualitative agreement with the few available and comparable experimental results. For instance, calculations confirmed trapping, alignments along the optical axis, and linear dependence of κ_z on laser power, as expected according to [7].

O. M. M. is grateful to P. G. Gucciardi, P. H. Jones, and A. C. Ferrari for fruitful discussions.

*borghese@ortica.unime.it
†marago@its.me.cnr.it

[1] A. Ashkin, J. M. Dziedzic, J. E. Bjorkholm, and S. Chu, Opt. Lett. **11**, 288 (1986).
[2] J. E. Molloy and M. F. Padgett, Contemp. Phys. **43**, 241 (2002).
[3] K. Svoboda and S. M. Block, Annu. Rev. Biophys. Biomol. Struct. **23**, 247 (1994).
[4] Special issue on Optical Micromanipulation, edited by N. Zheludev and E. Ozbay [J. Opt. A Pure Appl. Opt. **9**, 1 (2007)].
[5] A. Ashkin, *Optical Trapping and Manipulation of Neutral Particles Using Lasers* (World Scientific, Singapore, 2007).
[6] R. Agarwal, K. Ladavac, Y. Roichman, G. Yu, C. Lieber, and D. Grier, Opt. Express **13**, 8906 (2005).
[7] P. J. Pauzauskie, A. Radenovic, E. Trepagnier, H. Shroff, P. Yang, and J. Liphard, Nat. Mater. **5**, 97 (2006).
[8] Y. Nakayama, P. J. Pauzauskie, A. Radenovic, R. M. Onorato, R. J. Saykally, J. Liphardt, and P. Yang, Nature (London) **447**, 1098 (2007).
[9] S. Tan, H. A. Lopez, C. W. Cai, and Y. Zhang, Nano Lett. **4**, 1415 (2004).
[10] J. Plewa, E. Tanner, D. Mueth, and D. Grier, Opt. Express **12**, 1978 (2004).
[11] J. Zhang, H. I. Kim, C. H. Oh, X. Sun, and H. Lee, Appl. Phys. Lett. **88**, 053123 (2006).
[12] O. M. Maragò *et al.*, Physica E (Amsterdam) (to be published).
[13] P. Yang, Nature (London) **425**, 243 (2003).
[14] A. Thess *et al.*, Science **273**, 483 (1996).
[15] A. Rohrbach, Phys. Rev. Lett. **95**, 168102 (2005).
[16] F. Borghese, P. Denti, R. Saija, and M. A. Iatì, Opt. Express **15**, 11 984 (2007); **15**, 14 618(E) (2007).
[17] F. Borghese, P. Denti, R. Saija, and M. A. Iatì, Opt. Express **14**, 9508 (2006); **15**, 7005(E) (2007).
[18] J. D. Jackson, *Classical Electrodynamics* (Wiley, New York, 1975), 2nd ed.
[19] E. M. Rose, *Elementary Theory of Angular Momentum* (Wiley, New York, 1956).
[20] P. C. Waterman, Phys. Rev. D **3**, 825 (1971).
[21] R. Saija, M. A. Iatì, F. Borghese, P. Denti, S. Aiello, and C. Cecchi-Pestellini, Astrophys. J. **559**, 993 (2001).
[22] R. Saija, M. A. Iatì, P. Denti, F. Borghese, A. Giusto, and O. I. Sindoni, Appl. Opt. **42**, 2785 (2003).
[23] F. Borghese, P. Denti, and R. Saija, *Scattering from Model Nonspherical Particles* (Springer, Berlin, 2007), 2nd ed. Errata can be found at http://dfmtfa.unime.it/profs/borghese/ferdinandoborghese.html.
[24] L. Novotny and B. Hecht, *Principles of Nano-optics* (Cambridge University Press, Cambridge, England, 2006).
[25] A. Rohrbach and E. H. K. Stelzer, Appl. Opt. **41**, 2494 (2002).
[26] R. Saija, M. A. Iatì, P. Denti, F. Borghese, and O. I. Sindoni, Appl. Opt. **40**, 5337 (2001).
[27] M. I. Mishchenko, J. Quant. Spectrosc. Radiat. Transfer **70**, 811 (2001).